

Potential red-emission phosphor (Ca, Sr)(Mo, W)O₄:Eu³⁺, Y³⁺ and charge compensation impact on its luminescent property

FABIN CAO *, LUHONG WEI, LIAOSHA LI, XINGRONG WU

Anhui Provincial Key Laboratory of Metallurgical Engineering & Resources Recycling (Anhui University of Technology), Maanshan, Anhui, 243002, PR China

Eu³⁺-Y³⁺ co-doped (Sr_{0.88-x-1.5y}Ca_xEu_yY_{0.08})(Mo_{0.2}W_{0.8})O₄(x=0.20, 0.30, 0.40, 0.50, 0.60, 0.70. y=0.02, 0.04, 0.06, 0.08, 0.10, 0.12, 0.16, 0.20) were prepared by sol-gel method, and their crystal structures and luminescent properties were investigated. Through XRD, photoluminescence spectra analyses and powder size measurements, changing Ca²⁺ concentration, Eu³⁺ concentration and charge compensators components were performed for optimization its emission property. It was found that, with 2 mol% 0.6Li₂CO₃-0.4K₂CO₃ charge compensation, (Sr_{0.26}Ca_{0.5}Eu_{0.08}Y_{0.08})(Mo_{0.2}W_{0.8})O₄ possesses better emission property than the commercial phosphor Y₂O₃:Eu³⁺.

(Received March 23, 2014; accepted November 13, 2014)

Keywords: Charge compensators, Optical properties, Sol-gel method

1. Introduction

White-light-emitting diodes (LEDs) were known as the next generation of lighting sources due to their high efficiency and energy-saving properties and had already been introduced into the automobile industry, personal communication, displaying and illumination fields [1]. In 1996, the Nichia chemical company produced the first commercial white-LED, of which white light was produced by combining yellow-emitting yttrium aluminum garnet (YAG) with a blue-emitting phosphor chip [2]. Nowadays the white-LED with color rendering index 85 could satisfy the ordinary illumination requirements. [3] Nowadays mostly commercial red phosphors, such as CASN(CaAlSiN₃:Eu) and SCASN ((Sr,Ca)AlSiN₃:Eu), were dominated by Mitsubishi Chemical Corporation. However, these red phosphors couldn't meet some special requirements under UV or near UV excitation. Thus, in the past years, a series of molybdates phosphors had been synthesized. In order to meet the requirements of applications, the emission efficiency of these phosphors should be improved to some extent. For instance, the radius of W⁶⁺ ions (0.42 Å) close to those of Mo⁶⁺ ions, W⁶⁺ ions were introduced into the molybdates host materials for changing the structure of the sub-lattice surrounding the luminescent center ions, resulting into enhancing the emission property of luminescent center. In our previous research work, several kinds of red-emission phosphors based on tungstate-molybdate were fabricated by the solid-state methods [4-12]. However, the size of phosphor's particles was 20-30 μm, too large to be

beneficially applied in LEDs and plasma display panels. In addition, it was investigated for the ratio of WO₄²⁻/MoO₄²⁻ and the concentration of Y³⁺ ions in the host lattice affecting the emission characteristics of the phosphors. It was found that the optimum ratio of WO₄²⁻/MoO₄²⁻ and Y³⁺ concentration were 4:1 and 8 mol%, respectively.[12]

In this article, we described a series of (Sr_{0.88-x-1.5y}Ca_xEu_yY_{0.08})(Mo_{0.2}W_{0.8})O₄(x=0.20, 0.30, 0.40, 0.50, 0.60, 0.70. y=0.02, 0.04, 0.06, 0.08, 0.10, 0.12, 0.16, 0.20) prepared by sol-gel method and showed the concentration of Eu³⁺ and Ca²⁺ ions concentration affecting the emission intensity of the phosphors and the structure of host lattice. Furthermore, we discussed different kinds of charge compensators in affecting the emission characteristics, the particles size and the crystal structure of the phosphors.

2. Experimental

A series of red-emitting (Ca_xSr_{0.88-x-1.5y}Eu_yY_{0.08})(Mo_{0.2}W_{0.8})O₄ (x=0.20, 0.30, 0.40, 0.50, 0.60, 0.70. y=0.02, 0.04, 0.06, 0.08, 0.10, 0.12, 0.16, 0.20)(the amount of each phosphor, 5 mmol) phosphors were synthesized by sol-gel method. According to the chemical formulas, stoichiometric amount of yttrium oxide (Y₂O₃, purity 99.99%), europium oxide (Eu₂O₃, purity 99.99%), strontium carbonate(SrCO₃, AR) and calcium oxide(CaO, AR) were dissolved in 0.5 mol/L nitric acid (HNO₃, AR) 100 mL under vigorous stirring. The solution was heated at 65°C for 1 h (an excess of HNO₃ were removed by evaporation). 100 mL deionized water, Oxalic acid

($C_2H_2O_4 \cdot 2H_2O$, AR), ammonium molybdate ($(NH_4)_6Mo_7O_{24} \cdot 4H_2O$, AR), and ammonium tungstate ($(NH_4)_{10}H_2(W_2O_7)_6$, AR) was added to the solution. Oxalic acid acted as chelating agent for the metal ions and the molar ratio of ammonium molybdate and ammonium tungstate to oxalic acid was 1:2. The pH value of the final solution was adjusted to 7–8 by adding suitable amount of 0.05 mol/L ammonium hydroxide (NH_4OH , AR), and a clear solution was obtained after stirring for 15 minutes. This solution was heated in 90°C water bath to obtain a transparent light-brown gel and this gel was further dried at 110°C for 72 h. In air the dried gel was annealed at 900°C with stoichiometric amount of lithium carbonate/ sodium carbonate/ potassium carbonate (Li_2CO_3 / Na_2CO_3 / K_2CO_3 , AR) for 2 h to obtain the white phosphor powder. (All reagents were bought from Sinopharm Chemical Reagent Co., Ltd.).

The structures of the products were recorded by X-ray powder diffraction (XRD) employing $CuK\alpha$ radiation at 40kv and 250mA. A step size of $0.02^\circ(2\theta)$ was used with a scan speed of $4^\circ/\text{min}$. Excitation and emission spectra were measured by using a Hitachi F-4600 spectrometer equipped with a 150 W-xenon lamp under a working voltage of 550 V. The excitation and emission slits were set at 2.5 nm and scanning speed was 1200nm/min. The size of phosphor's particles was determined by a Rise-2006 laser grain size analyzer (Jinan Rise Science & Technology Co., Ltd., Jinan City, Shandong Province, P.R.China, measuring range 0.05–800 μm , measuring accuracy 0.001 μm). [13]All the measurements were performed at room temperature.

3. Results and discussion

Fig. 1 depicts the XRD patterns of $(Sr_{0.38}Ca_{0.50}Y_{0.08})(Mo_{0.2}W_{0.8})O_4$ (SCYMW)(c), $(Sr_{0.38}Ca_{0.50}Eu_{0.08})(Mo_{0.2}W_{0.8})O_4$ (SCEMW)(b) and $(Sr_{0.26}Ca_{0.50}Eu_{0.08}Y_{0.08})(Mo_{0.2}W_{0.8})O_4$ (SCEYMW)(a). It is found that SCYMW, SCEMW and SCEYMW all own scheelite phases, consistent to standard $CaMoO_4$ crystal structure, viz. the characteristic peaks of the tetragonal crystal structure with space group of $I4_1/a(88)$. And no CaO , $SrCO_3$, WO_3 , MoO_3 , Eu_2O_3 and Y_2O_3 corresponding characteristic peaks emerge.

Fig. 2 presents XRD patterns of SCEYMW with no charge compensators or 2 mol% $0.6Li_2CO_3 - 0.4K_2CO_3$. It is investigated that the crystal structure of the phosphor is consistent with $CaMoO_4$ standard pattern (JCPDS 29-0351) with charge compensators or not. The full width at half maximum (FWHM) of the main peak is 0.0957 deg. with 2 mol% $0.6Li_2CO_3 - 0.4K_2CO_3$ used as charge compensators and the FWHM is 0.1583 deg. without charge compensators. It is indicated that the crystallinity of the phosphor increases with appropriate amount of charge compensators introduced into the host [14].

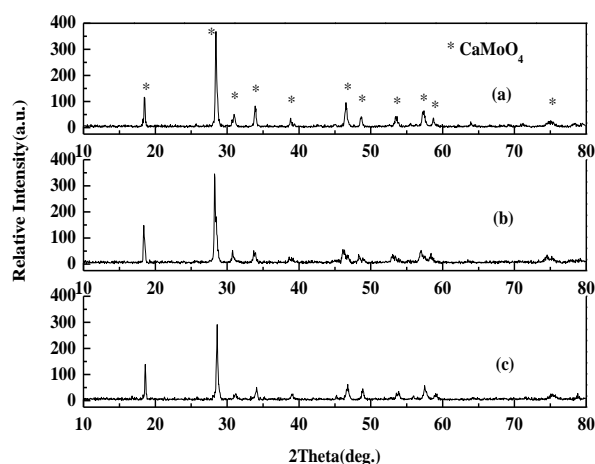


Fig. 1. XRD patterns of SCEYMW (a), SCEMW (b) and SCYMW (c).

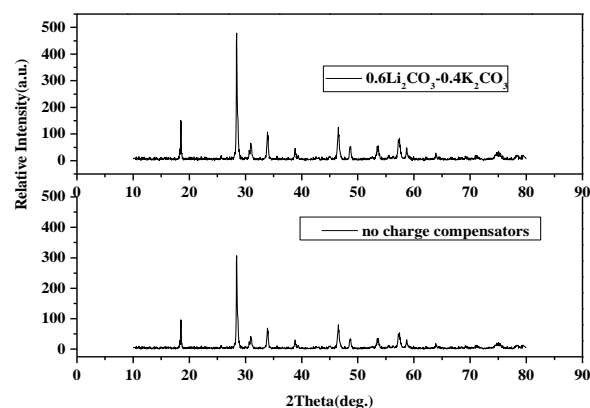


Fig. 2. XRD patterns of SCEYMW with no charge compensators or 2 mol% $0.6Li_2CO_3 - 0.4K_2CO_3$.

Activators concentration is an important factor in affecting the luminescent property of phosphors in the experiment. Fig. 3 shows the effect of Eu^{3+} ions concentration on emission intensity of $(Sr_{0.38-1.5x}Ca_{0.5}Eu_xY_{0.08})(Mo_{0.2}W_{0.8})O_4$ ($x = 0.02, 0.04, 0.06, 0.08, 0.10, 0.12, 0.16, 0.20$) at 616 nm under 394 nm or 465 nm excitation. With Eu^{3+} concentration increasing, its emission intensity enhances. Eu^{3+} concentration being 8mol%, its emission intensity is the strongest, up to 8016 a.u. When Eu^{3+} ions concentration exceeds 8 mol%, the emission intensity increases indistinctively with Eu^{3+} concentration increasing. In the same conditions, the effect of Eu^{3+} concentration on the emission intensity of the phosphor abides by the same law under 465 nm as 394 nm excitation. It is indicated that concentration quenching of Eu^{3+} ions occurs in the SCEYMW luminescent system.

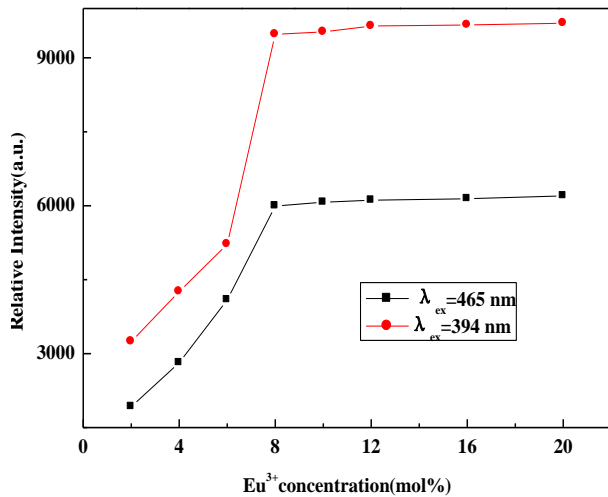


Fig. 3. The emission intensity of (Sr_{0.38-1.5x}Ca_{0.5}Eu_xY_{0.08})(Mo_{0.2}W_{0.8})O₄ ($x = 0.02, 0.04, 0.06, 0.08, 0.10, 0.12, 0.16, 0.20$) (excited by 394 nm or 465 nm) with different Eu³⁺ concentration.

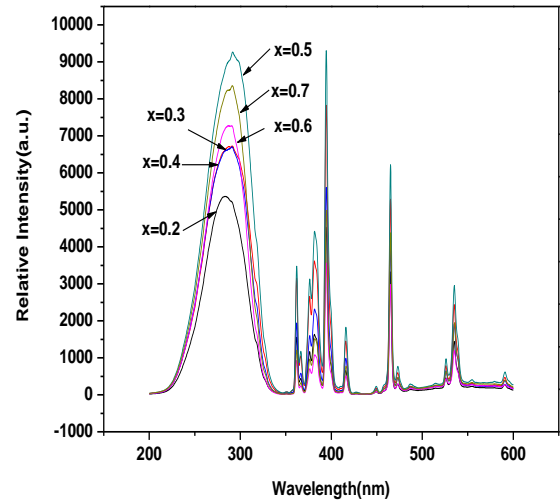


Fig. 4. The excitation spectra of (Sr_{0.76-x}Ca_xEu_{0.08}Y_{0.08})(Mo_{0.2}W_{0.8})O₄ ($x = 0.2, 0.3, 0.4, 0.5, 0.6, 0.7$) monitored at 616 nm.

Table 1. The position and intensity of excitation peaks of SCEYMW at ambient temperature. ^a.

Transitions	The position of excitation maximum (nm)	The intensity of excitation maximum (a.u.)
O ²⁻ →Mo ⁶⁺ /W ⁶⁺	291.6	9265
⁷ F ₀ → ⁵ D ₄	362	3479
⁷ F ₁ → ⁵ D ₄	366.6	1175
⁷ F ₀ → ⁵ G ₄	376.2	3127
⁷ F ₀ → ⁵ G ₂	381.8	4423
⁷ F ₀ → ⁵ L ₆	394.4	9306
⁷ F ₀ → ⁵ D ₃	416	1824
⁷ F ₁ → ⁵ D ₃	427.2	74.1
⁷ F ₃ → ⁵ D ₃	449.4	225.7
⁷ F ₀ → ⁵ D ₂	465	6223
⁷ F ₁ → ⁵ D ₂	473.2	770.9
⁷ F ₂ → ⁵ D ₂	486.6	288.3
⁷ F ₃ → ⁵ D ₂	514.8	310.8
⁷ F ₂ → ⁵ D ₁	526.2	971.6
⁷ F ₀ → ⁵ D ₁	535.2	2957

^a Under 616 nm monitoring.

Fig. 4 depicts the excitation spectra of (Sr_{0.38-1.5x}Ca_{0.5}Eu_xY_{0.08})(Mo_{0.2}W_{0.8})O₄ ($x = 0.02, 0.04, 0.06, 0.08, 0.10, 0.12, 0.16, 0.20$) monitored at 616 nm. In the excitation spectra, at 300 nm or so, there is one strong broad band with the same shape. In general, the broad band is attributed to O²⁻→Mo⁶⁺/W⁶⁺/Eu³⁺ charge transition. But in fact, O²⁻→Eu³⁺ charge transition can be neglected for Eu³⁺ concentration (8 mol %) is much lower than Mo⁶⁺ concentration/W⁶⁺ concentration (20 mol%/ 80 mol %). In addition, the symmetry of the broad band is good and there is little change that three peaks overlap together forming the symmetric broad band. So the broad band (main peak at 291.6 nm) is ascribed to O²⁻→Mo⁶⁺/W⁶⁺ transitions, seen in Table 1. From 350 nm to 550nm in the excitation spectra, all samples own intrinsic characteristic narrow bands attributed to 4f-4f transition, six strong narrow bands derived from ⁷F₀→⁵D₄(362 nm), ⁷F₀→⁵G₄(376.2 nm), ⁷F₀→⁵G₂(381.8 nm), ⁷F₀→⁵L₆(394 nm), ⁷F₀→⁵D₂(465 nm) and ⁷F₀→⁵D₁(535 nm), respectively, and eight weak peaks attributed to ⁷F₁→⁵D₄(366.6 nm), ⁷F₀→⁵D₃(416 nm), ⁷F₁→⁵D₃(427.2 nm), ⁷F₃→⁵D₃(449.4 nm), ⁷F₁→⁵D₂(473.2 nm), ⁷F₂→⁵D₂(486.6 nm), ⁷F₃→⁵D₂(514.8 nm) and ⁷F₂→⁵D₁(526.2 nm).

Table 2. The position and intensity of emission peaks of SCEYMW at ambient temperature.

Transitions	The position of emission maximum (nm)	The intensity of emission maximum (a.u.)	
⁵ D ₀ → ⁷ F ₁	592.2	933 ^a	595 ^b
⁵ D ₀ → ⁷ F ₂	616.2	9476 ^a	5995 ^b
⁵ D ₀ → ⁷ F ₃	655.2	202.2 ^a	133.1 ^b
⁵ D ₀ → ⁷ F ₄	702.8	693 ^a	450 ^b

^a Under 394 nm excitation. ^b Under 465 nm excitation.

Under 394 nm and 465 nm excitation, respectively, the emission spectra of $(\text{Sr}_{0.76-x}\text{Ca}_x\text{Eu}_{0.08}\text{Y}_{0.08})(\text{Mo}_{0.2}\text{W}_{0.8})\text{O}_4$ ($x=0.2, 0.3, 0.4, 0.5, 0.6, 0.7$) samples are shown in Fig. 5 and Fig. 6. From 550 nm to 750 nm in the emission spectra, four emission peaks locate at 592.2 nm, 616.2 nm, 655.2 nm and 702.8 nm, attributed to ${}^5\text{D}_0 \rightarrow {}^7\text{F}_J$ ($J=1, 2, 3, 4$), respectively, in Table 2. The main emission peak locates at 616 nm and the others peaks are too weak peaks, which is beneficial to the phosphors with good color purity. In the emission spectra, ${}^5\text{D}_0 \rightarrow {}^7\text{F}_{1,3}$ transitions at 592 nm and 655.2 nm, respectively, are magnetic dipole transition and ${}^5\text{D}_0 \rightarrow {}^7\text{F}_{2,4}$ transitions at 616.2 nm and 702.8 nm, respectively, are electric dipole transition. ${}^5\text{D}_0 \rightarrow {}^7\text{F}_2$ transition is much stronger than ${}^5\text{D}_0 \rightarrow {}^7\text{F}_1$ transition. ${}^5\text{D}_0 \rightarrow {}^7\text{F}_1$ transition (Eu^{3+} ions) waves a little in different host materials and Eu^{3+} ions should occupy the inversion symmetry position. And the value of ${}^5\text{D}_0 \rightarrow {}^7\text{F}_2$ transition / ${}^5\text{D}_0 \rightarrow {}^7\text{F}_1$ transition (SCEYMW, 10.2 at 394 nm, 10.1 at 465 nm) is acted as the standard of emission characteristics of phosphors. Although the emission peaks of molybdates or tungstates cannot be observed in Fig. 5 and Fig. 6, the excitation peaks attributed to molybdates or tungstates appear in Fig. 4. It means that the energy absorbed by $\text{WO}_4^{2-}/\text{MoO}_4^{2-}$ ions clusters has been transferred to Eu^{3+} ions.

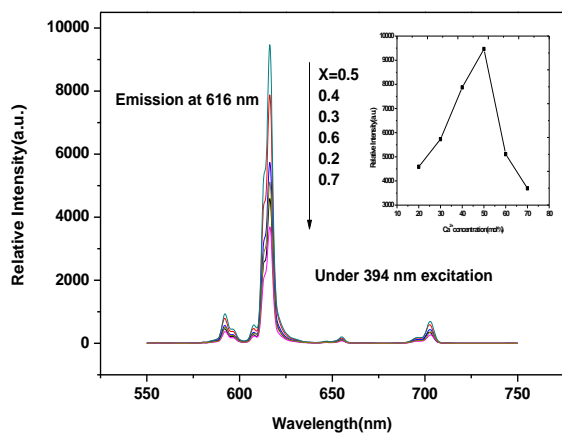


Fig. 5. The emission spectra of $(\text{Sr}_{0.76-x}\text{Ca}_x\text{Eu}_{0.08}\text{Y}_{0.08})(\text{Mo}_{0.2}\text{W}_{0.8})\text{O}_4$ ($x=0.2, 0.3, 0.4, 0.5, 0.6, 0.7$) under 394nm excitation.

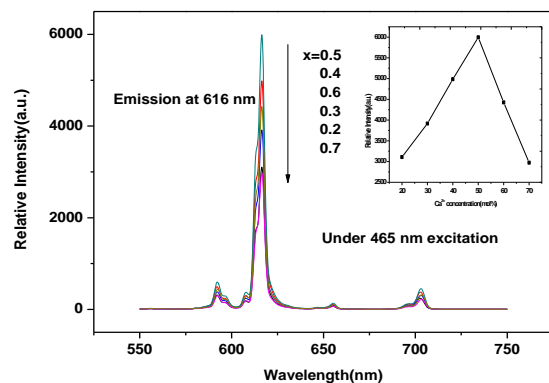


Fig. 6. The emission spectra of $(\text{Sr}_{0.76-x}\text{Ca}_x\text{Eu}_{0.08}\text{Y}_{0.08})(\text{Mo}_{0.2}\text{W}_{0.8})\text{O}_4$ ($x=0.2, 0.3, 0.4, 0.5, 0.6, 0.7$) under 465nm excitation.

To Eu^{3+} ions activating phosphors, the intensity of charge transition band is stronger than of 4f-4f transition of Eu^{3+} ions in the excitation spectra. This view is validated in the references [8, 9, 15-18]. But, in the experiment, the excitation spectra observed are not consistent with the above view. It is probable that the energy of $\text{O}^{2-} \rightarrow \text{Mo}^{6+}/\text{W}^{6+}$ charge transition band can be effectively transferred to the luminescent center- Eu^{3+} ions determined by the environment of luminescent center ions (Eu^{3+} ions).

Tungstates and molybdates can supply the conditions favorable for optimization of luminescent characteristics of Eu^{3+} ions, so they are usually selected as host materials. For their strong charge transfer properties, they can be employed to enhance energy transfer efficiency in NUV [8, 9]. In the same argument, $\text{Sr}^{2+}/\text{Ca}^{2+}$ concentration in the host is an important factor in affecting the environment of luminescent center ions (Eu^{3+} ions). Fig. 4 depicts the excitation spectra of $(\text{Sr}_{0.76-x}\text{Ca}_x\text{Eu}_{0.08}\text{Y}_{0.08})(\text{Mo}_{0.2}\text{W}_{0.8})\text{O}_4$ ($x=0.2, 0.3, 0.4, 0.5, 0.6, 0.7$) doped different Ca^{2+} concentration under 394 nm and 465 nm excitation, respectively, which can be divided into two stages. In the first stage, with Ca^{2+} concentration increasing, the emission intensity of the phosphors enhances and it is up to 9461 a.u. and 5995 a.u., respectively, when Ca^{2+} concentration is 50 mol%. In the second stage, with Ca^{2+} concentration increasing, the emission intensity of the phosphor decreases sharply. It is interesting that, with Ca^{2+} concentration changing, under 394 nm and 465 nm excitation, respectively, the emission intensity of ${}^5\text{D}_0 \rightarrow {}^7\text{F}_2$ transition abides by the same laws. All these may be related to the characteristics of molybdates and tungstates used as the host. By this method, the absorption intensity of the phosphor can be tunable in the NUV and blue light fields so the phosphor can well match UV-LED and Blue-LED chips.

Based on the optimum Ca^{2+} and Eu^{3+} concentration, SCEYMW phosphors are prepared by 5 types of charge compensators. For molybdates and tungstates are both linear spectra, it is seen that adding charge compensators in the host cannot shift their emission spectra and can only affect their emission intensity in Fig. 7 and Fig. 8. So we only discuss the effect of charge compensators on the emission intensity and particle size of the phosphor.

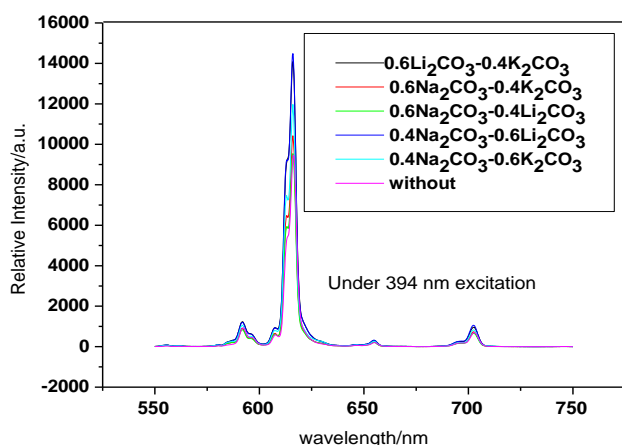


Fig. 7. The emission spectra of SCEYMW with different kinds of charge compensators (amount used, 2 mol%) under 394 nm excitation.

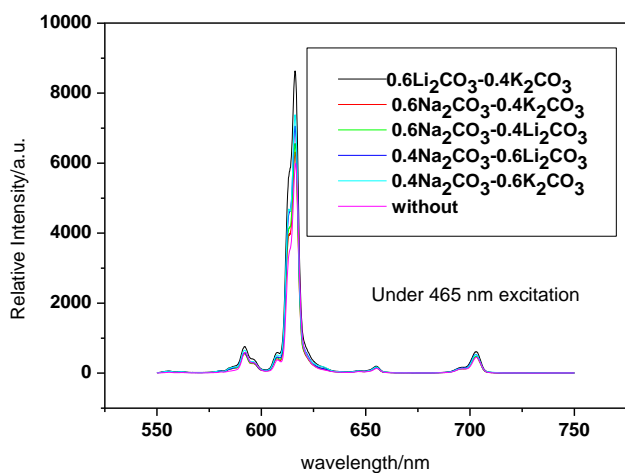


Fig. 8. The emission spectra of SCEYMW with different kinds of charge compensators (amount used, 2 mol%) under 465 nm excitation.

Table 3. The average particle size of SCEYMW synthesized with 2 mol% charge compensators.

charge compensators	Emission intensity (a.u.) at 616 nm	Average particle size(μm)
no	14434 ^a , 5995 ^b	5.05
0.6Li ₂ CO ₃ -0.4K ₂ CO ₃	14049 ^a , 8636 ^b	3.10
0.6Na ₂ CO ₃ -0.4K ₂ CO ₃	11718 ^a , 7382 ^b	3.55
0.6Na ₂ CO ₃ -0.4Li ₂ CO ₃	10421 ^a , 7061 ^b	3.82
0.4Na ₂ CO ₃ -0.6Li ₂ CO ₃	9536 ^a , 6561 ^b	4.03
0.4Na ₂ CO ₃ -0.6K ₂ CO ₃	9476 ^a , 6325 ^b	4.25

^aUnder 394 nm excitation. ^bUnder 465 nm excitation.

Charge compensators play an important role in affecting the emission ability of the preparation of SCEYMW crystal phosphors. With 2 mol% 5 types of charge compensators, respectively, incorporated into SCEYMW, the emission intensity and average particle size of the phosphors obtained are listed in Table 3. For instance, with 2 mol% 0.6Li₂CO₃-0.4K₂CO₃ used as charge compensators, the average particle size of the phosphor is 3.1 μm and its emission intensity enhances 152% compared to SCEYMW without charge compensators. It is indicated that 2 mol% 0.6Li₂CO₃-0.4K₂CO₃ is the optimum charge compensators. Due to the charge compensators employed, SCEYMW has the optimum crystallization and the luminescent center ions exist in the ideal circumstances, which is advantageous to exhibit better optical characteristics. Although the emission intensity and the average particle size do not necessarily exist in a correlation, the phosphors have the special requirement for white LED application and three factors must be considered. Above all, it should be considered for the emission intensity of the phosphor. In general, the phosphor should own better brightness output, and should match the blue or UV LED chips. Secondly, average particle size. The average particle size of the phosphor is less than 8 μm, too small or too big reducing the efficiency of light conversion. Last but not least, the phosphor should possess good physical property, chemical stability and moisture resistance, not reaction with semiconductor chips. Based on the above three factors combined with the experimental results, 2 mol% 0.6Li₂CO₃-0.4K₂CO₃ are chosen to be employed as charge compensators. Through charge compensation, SCEYMW phosphors can be improved pronounced. Its average particle size is 3.1 μm (in Table 3). Compared with the commercial Y₂O₂S:Eu³⁺(1.25, 0.6872 and x=0.667, y=0.326) phosphor in Table 4, it is advantageous to apply in LED illumination and LED display for the relative emission intensity, decay time and color coordinates of SCEYMW charge compensated(1.52, 0.5288 and x=0.662, y=0.330).

Table 4. Relative emission intensities, decay times and CIE color coordinates for SCEYMW phosphors with no charge compensators or 2 mol% 0.6Li₂CO₃-0.4K₂CO₃ (λ_{ex}=246 nm for Y₂O₂S:Eu³⁺ and λ_{ex}=394 nm for SCEYMW).

Phosphor	Relative emission intensity	Decay time (ms)	CIE color coordinates
SCEYMW	1	0.5289	x=0.661, y=0.330
Y ₂ O ₂ S:Eu ³⁺	1.25	0.6872	x=0.667, y=0.326
SCEYMW'	1.52	0.5288	x=0.662, y=0.330

^aSCEYMW' means SCEYMW phosphors after charge compensation by 2 mol% 0.6Li₂CO₃-0.4K₂CO₃

4. Conclusions

Through optimizing Ca^{2+} concentration and Eu^{3+} concentration, a red-emitting $(\text{Sr}_{0.26}\text{Ca}_{0.5}\text{Eu}_{0.08}\text{Y}_{0.08})(\text{Mo}_{0.2}\text{W}_{0.8})\text{O}_4$ phosphor was obtained by sol-gel method. It can be excited efficiently by 394 nm and 465 nm, its main emission peak at 616 nm. With 2 mol% $0.6\text{Li}_2\text{CO}_3\text{-}0.4\text{K}_2\text{CO}_3$ used as charge compensators introduced into the host, the crystallization degree of $(\text{Sr}_{0.26}\text{Ca}_{0.5}\text{Eu}_{0.08}\text{Y}_{0.08})(\text{Mo}_{0.2}\text{W}_{0.8})\text{O}_4$ and its relative emission intensity were improved, and its particle size was up to 3.1 μm . Compared with the commercial $\text{Y}_2\text{O}_3\text{:Eu}^{3+}$ (1.25, 0.6872 and $x=0.667$, $y=0.326$) phosphor, it is advantageous to apply in LED illumination and LED display for the relative emission intensity, decay time and color coordinates of SCEYMW charge compensated (1.52, 0.5288 and $x=0.662$, $y=0.330$).

Acknowledgment

The work was supported by Natural Science Foundation for Anhui Provincial Education Agency in PR China (Grant No. KJ2011Z032), Natural Science Foundation for Anhui Provincial Science and Technology Agency (Grant No. 1408085ME78) in PR China and National Natural Science Foundation for PR China (No. 51274006).

References

- [1] F. K. Yam, Z. Hassan, *Microelectronics J.* **36**, 129 (2005).
- [2] J. Liu, J. Y. Sun, C. S. Shi, *Chem Online* **68**, 417 (2005).

- [3] N. Narendran, N. Maliyagoda, L. Deng, P. Richard, *SPIE Proc Ser* **4445**, 137 (2001).
- [4] F. B. Cao, L. S. Li, Y. W. Tian, W. X. Rong, Y. J. Chen, L. J. Xiao, *Appl. Spectrosc.* **64**, 1298 (2010).
- [5] F. B. Cao, Y. W. Tian, Y. J. Chen, L. J. Xiao, Q. Wu, *J. Lumin* **129**, 585 (2009).
- [6] F. B. Cao, Y. W. Tian, Y. J. Chen, L. J. Xiao, Q. Wu, *J. Alloy. Compd.* **475**, 387 (2009).
- [7] F. B. Cao, Y. W. Tian, Y. J. Chen, L. J. Xiao, Y. Y. Liu, L. K. Li, *Mater. Sci. Semicon. Proc.* **12**, 94 (2009).
- [8] F. B. Cao, Y. W. Tian, Y. J. Chen, L. J. Xiao, L. K. Li, *Appl. Phys. B-Lasers O.* **48**, 417 (2009).
- [9] Y. J. Chen, F. B. Cao, Y. W. Tian, L. J. Xiao, L. K. Li, *Physica B.* **405**, 435 (2010).
- [10] F. B. Cao, Y. W. Tian, Y. J. Chen, L. J. Xiao, L. K. Li, *Appl. Spectrosc.* **64**, 241 (2010).
- [11] F. B. Cao, Y. W. Tian, L. S. Li, Y. J. Chen, L. J. Xiao, *J. Mater. Sci.: Mater. Electron* **22**, 510 (2011).
- [12] F. B. Cao, Y. W. Tian, Y. J. Chen, L. J. Xiao, Y. Y. Liu, *J. Nanosci. Nanotechno.* **10**, 2060 (2010).
- [13] F. Storti, F. Balsamo, *Solid Earth* **1**, 25 (2010).
- [14] J. L. Yang, Z. Wang, *J. Chin. Rare Earth Soc.* **28**, 536 (2010).
- [15] C. H. Chiu, M. F. Wang, C. S. Lee, T. M. Chen, *J. Solid Stat. Chem.* **180**, 619 (2007).
- [16] Z. L. Wang, H. B. Liang, L. Y. Zhou, H. Wu, M. L. Gong, Q. Su, *Chem. Phys. Lett.* **412**, 313 (2005).
- [17] X. X. Wang, Y. L. Xian, J. X. Shi, Q. Su, M. L. Gong, *Mater. Sci. Eng. B* **140**, 69 (2007).
- [18] N. Narendran, Y. Gu, J. P. Freyssonier, H. Yu, L. Deng, *Cryst. Growth* **268**, 449 (2004).

*Corresponding author: fbcao@ahut.edu.cn
yjsun7410@aliyun.com